Analysis of deformation of mistuned bladed disks with friction and random crystal anisotropy orientation using gradient-based polynomial chaos expansion

Article (Accepted Version)

Proceedings of ASME Turbo Expo 2018: Turbomachinery Technical Conference and Exposition
GT2018
June 11-15, 2018, Oslo, Norway

GT2018-76566

ANALYSIS OF DEFORMATION OF MISTUNED BLADED DISKS WITH FRICTION AND RANDOM CRYSTAL ANISOTROPY ORIENTATION USING GRADIENT-BASED POLYNOMIAL CHAOS EXPANSION

Rahul Rajasekharan
School of Engineering and Informatics
University of Sussex
United Kingdom
Email: R.Rajasekharan-Nair@sussex.ac.uk

E. P. Petrov
School of Engineering and Informatics
University of Sussex
United Kingdom
Email: Y.Petrov@sussex.ac.uk

ABSTRACT

Single crystal blades used in high pressure turbine bladed disks of modern gas-turbine engines exhibit material anisotropy. In this paper the sensitivity analysis is performed to quantify the effects of blade material anisotropy orientation on deformation of a mistuned bladed disk under static centrifugal load. For a realistic, high fidelity model of a bladed disk both: (i) linear, and (ii) non-linear friction contact conditions at blade roots and shrouds are considered. The following two kinds of analysis are performed: (i) local sensitivity analysis, based on first order derivatives of system response w.r.t design parameters, and (ii) statistical analysis using polynomial chaos expansion. The polynomial chaos expansion is used to transfer the uncertainty in random input parameters to uncertainty in static deformation of the bladed disk. An effective strategy, using gradient information, is proposed to address the "curse of dimensionality" problem associated with statistical analysis of realistic bladed disk.

ABBREVIATIONS

LSA	Local Sensitivity Analysis
GSA	Global Sensitivity Analysis
CS	Coordinate System
FE	Finite Element
PCE	Polynomial Chaos Expansion
MCS	Monte Carlo Simulation
gradPCE	gradient based Polynomial Chaos Expansion
CP	Collocation point
STD	Standard deviation

NOMENCLATURE

α, β, ζ	Crystal anisotropy angles
$\boldsymbol{\sigma}$	Cauchy stress tensor
$\boldsymbol{\varepsilon}$	Strain tensor
$\mathbf{S}$	Material Compliance matrix
$\mathbf{E}$	Material Elasticity matrix
$\mathbf{T}$	Coordinate transformation matrix
$\boldsymbol{K}$	Global stiffness matrix
$\boldsymbol{k}^e$	Element stiffness matrix
$\boldsymbol{r}$	Rotation vector defining crystal axis
$\boldsymbol{F}_{nln}$	Non-linear force vector
$\boldsymbol{P}$	Static force vector
ξ	Random variable
y	Stochastic function
n	Dimension of random space
p	Order of polynomial chaos expansion
ψ	Polynomial basis function
ρ	Probability density function

1 INTRODUCTION

1.1 Background and motivation

The prediction of deformation and stress fields of bladed disks under various mechanical and thermal loads is a challenging task in the design of gas turbine engines. The response of these structures to static and dynamic loading is dependent on multitude of geometric, material and loading parameters. The values of some of these parameters are uncertain especially when

taking into account the varying operating conditions of a gas turbine engine. To ensure the safe operation of the gas turbine engine, it is essential to assess the deformation of the structure accurately in presence of the uncertainty in input design parameters.

The nickel–based–alloy blades in high pressure turbine stages of modern gas turbine engines are often monocrystalline and the crystallographic orientation of the monocrystal influences the mechanical properties of the blades[1]. The scatter in crystal orientations due to inaccuracies in manufacturing process of single crystal blades results in the scatter in material properties of the blades. For designing a robust bladed disk, it is vital to quantify the effects of uncertainty in crystal orientations on deformation of the structure under different operational loads.

For a mistuned bladed disk, where blade properties has scatter due to unavoidable inaccuracies in manufacturing, significant difference in displacements and stresses between individual blades in a bladed disk is possible. To maximize the efficiency of gas-turbine engines, clearance between the blades and turbine casing must be minimized to reduce tip leakage. Modern gas-turbine engines use an abradable material seal which allows the formation of an optimal gap between blades and casing during the initial runs. Even though this technique has proved to be effective in minimizing the radial gap, there are two main concerns associated with it: (i) the possibility of the abradable material sticking to the blades, thereby, inducing turbulence in gas flow, and (ii) the phenomenon of blade wear due to friction between blades and abradable material [2]. However for a mistuned bladed disk with significant scatter in blade mechanical properties, each blade will have marginally different radial elongation which then precludes the possibility of creating an optimal gap. In this case, the blade with largest radial elongation will determine the amount of abradable material removed, thereby, creating a suboptimal tip-casing gap for other blades in the bladed disk.

To minimize the amount of abradable material removed and to maintain optimal tip-casing gap for all blades, there is a need to quantify the scatter in static deformation of bladed disks due to scatter in material properties of the blades.

Few investigations on the effects of blade material anisotropy orientation on different properties of the blades are available in the literature. Kaneko [3], Manetti et. al. [4] and Wen et. al. [5] investigated the effects of variation in crystal orientation on natural frequencies of blades. In his study, Kaneko [3] used a plate geometry to model the blade and the results indicated that the variations in three orientation angles, defining the crystal orientation, has different effects on natural frequencies of the blade. Savage [6] investigated the effects of crystal orientation on elastic stresses in single crystal blades. While Arakere et. al. [7] investigated the effects of crystal orientation on fatigue life of bladed disk, Weiss et. al. [8] investigated the effects of crystal orientation on the life time of monocrystal blades determined by the low-cycle fatigue and creep damages using probabilistic finite element analysis based on Monte-Carlo-Simulation (MCS) techniques.

The aim of sensitivity analysis is to obtain a measure of output variation with respect to system input parameter variations [9]. While a limited number of literature dealing with sensitivity analysis of bladed disks in gas turbine engines is available, sensitivity analysis of static deformation of bladed disks w.r.t scatter in material anisotropy orientation of single crystal blades are not available. Petrov [10] derived analytical expressions for first and second order sensitivity derivatives, w.r.t parameters of friction contact interface, frequency and level of excitation forces for non-linear forced response of a structure. In Ref.[11], he used sensitivity derivatives to calculate uncertainty ranges and stochastic characteristics of forced response for nonlinear vibrations of bladed disks with friction and gap contact interfaces. Panunzio et. al. [12] used polynomial chaos expansion (PCE) to study the effects of uncertainty in tip-casing gap on non-linear normal modes of turbine blades. Considering the modal stiffness of blades as random variables, Sinha [13] obtained the statistics of forced response for mistuned bladed disks using PCE.

The sensitivity analysis could be generally divided into two groups; (i) local sensitivity analysis (LSA), and (ii) global sensitivity analysis (GSA). The aim of LSA is to calculate sensitivity coefficients, i.e. first or higher order derivatives of response with respect to design parameters, at a chosen point in the domain of variation of the design variables. GSA studies the variability of system response w.r.t variation in design parameters and their higher order interactions over the entire domain of variation of the design variables.

A study of available literature on LSA shows that following approaches have been used to evaluate the derivatives: (i) finite difference method [14]: which is easy to implement but suffers from high computational cost, (ii) direct differentiation method: which offers high accuracy at low computational cost, (iii) adjoint differentiation method: which uses Lagrange multiplier to simplify the calculation of derivatives [15] and (iv) semi-analytical method: which reduces the complexity in implementation associated with direct and adjoint method by allowing some of the derivatives to be evaluated using finite difference [16].

The objective of GSA is to quantify the variation in system output w.r.t to variations in input parameters over the domain of variation. Monte Carlo simulation (MCS) [17], variance based decomposition [18], stochastic finite element method [19], polynomial chaos expansion [20] are some of the methods available to perform GSA. MCS is a sampling based technique which relies on multiple executions of the numerical model to generate a mapping between random input parameters and model outputs. The accuracy of MCS is proportional to the square root of the number of realizations used to characterize the stochastic response, and therefore, computationally inefficient especially for analysis of mistuned bladed disks where non-linearities due to

friction contacts are included.

As a tool for uncertainty quantification of dynamic systems, PCE has been studied extensively [21, 22]. The main feature of PCE is the decomposition of output response into a linear combination of deterministic and stochastic components. The computational effort in obtaining PCE is associated with calculation of coefficients in the expansion based on finite number of realizations of deterministic FE model of the bladed disks.

2 OBJECTIVE AND SCOPE

In this paper the effects of scatter in crystal orientation of single crystal blades on deformation and stress fields of realistic bladed disks under static centrifugal load are investigated. Sensitivity of displacements and stresses based on first order derivatives for linear and non-linear bladed disks with friction contacts are calculated. The insight gained from sensitivity analysis is used to device a strategy for efficient estimation of statistics for stochastic response of mistuned bladed disk. The use of PC expansion as a computationally efficient alternative to MCS is investigated. A realistic bladed disk model for the following two cases, (i) linear bladed disk and (ii) non-linear bladed disk, are used for the investigation. The improvement in computational efficiency associated with the use of gradient values in calculating PC expansion coefficients and its influence on convergence of statistical characteristics are investigated.

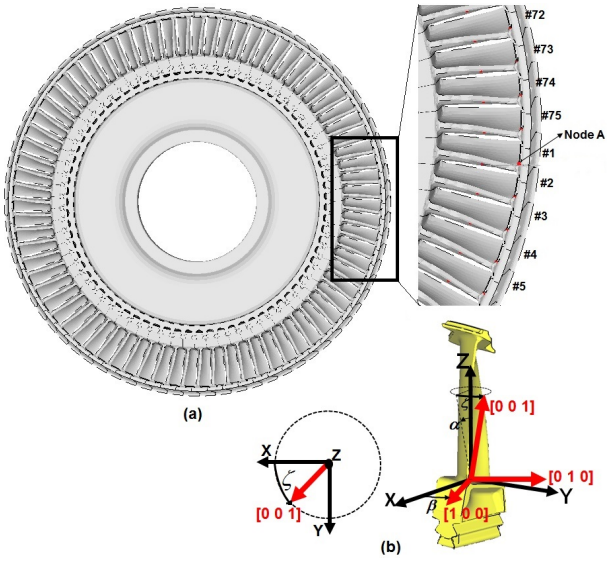

FIGURE 1: Geometry of (a) full bladed–disk & (b) a single blade showing crystallographic axis orientation.

3 ANALYSIS METHOD

3.1 Modelling of bladed disks with anisotropic blades

Fig. 1a shows a realistic bladed disk model with 75 blades having random crystal orientations. The rotation of crystal axis is represented by coordinate system (CS) rotation, defined by three angles, α, β and ζ as shown in Fig.1b

The elastic stress–strain relationship for orthotropic materials is given by Eq.(1)

$$\{\boldsymbol{\varepsilon}\} = [\mathbf{S}]\{\boldsymbol{\sigma}\} \tag{1}$$

where, $\boldsymbol{\sigma}$ and $\boldsymbol{\varepsilon}$ are stress tensor and strain tensor in the crystal CS and the material compliance matrix, $[\mathbf{S}]$, expressed in the CS coinciding with the material anisotropy axes is written as:

$$[\mathbf{S}] = \begin{bmatrix} \frac{1}{E_x} & \frac{-\nu_{xy}}{E_x} & \frac{-\nu_{xz}}{E_x} & 0 & 0 & 0 \\ \frac{-\nu_{yx}}{E_y} & \frac{1}{E_y} & \frac{-\nu_{yz}}{E_y} & 0 & 0 & 0 \\ \frac{-\nu_{zx}}{E_z} & \frac{-\nu_{zy}}{E_z} & \frac{1}{E_z} & 0 & 0 & 0 \\ 0 & 0 & 0 & \frac{1}{G_{yz}} & 0 & 0 \\ 0 & 0 & 0 & 0 & \frac{1}{G_{xz}} & 0 \\ 0 & 0 & 0 & 0 & 0 & \frac{1}{G_{xy}} \end{bmatrix} \tag{2}$$

where, ν is Poisson's ratio, E is Young's modulus and G is shear modulus.

In order to perform FE analysis of a bladed disk, the stress-strain relationship (Eq.1) has to be transformed in a global CS. The coordinate transformation for stresses in crystal coordinate system to stresses in global CS is given by Eq.(3)

$$\{\boldsymbol{\sigma}'\} = [\mathbf{T}_\sigma]\{\boldsymbol{\sigma}\} \tag{3}$$

Similarly, strains could be transformed:

$$\{\boldsymbol{\varepsilon}'\} = [\mathbf{T}_\varepsilon]\{\boldsymbol{\varepsilon}\} \tag{4}$$

where, $\boldsymbol{\sigma}'$ and $\boldsymbol{\varepsilon}'$ are stresses and strains in global CS, $[\mathbf{T}_\sigma]$ and $[\mathbf{T}_\varepsilon]$ are transformation matrices for stress and strain respectively. These matrices are formed from direction cosines of blade anisotropy CS while allowing for orientation of blade stacking axis in the bladed disk. From Eqs.(1), (3) and (4), the compliance matrix in global CS could be written as in Eq.(5)

$$[\mathbf{S}'] = [\mathbf{T}_\varepsilon][\mathbf{S}][\mathbf{T}_\sigma]^{-1} \tag{5}$$

Similarly, the elasticity matrix is given by Eq.(6)

$$[\mathbf{E}'] = [\mathbf{T}_\varepsilon][\mathbf{E}][\mathbf{T}_\sigma]^{-1} \tag{6}$$

For non-linear static problem, the solution is obtained by solving the governing equation of the bladed disk:

$$\boldsymbol{K}(\boldsymbol{r}_j)\boldsymbol{x} + \boldsymbol{F}_{nln}(\boldsymbol{x}) = \boldsymbol{P},\ j = 1, \ldots, N_B \tag{7}$$

where, $\boldsymbol{r}_j = \{r_x, r_y, r_z\}$ is the rotation vector defining the orientation of crystallographic axis of j^{th} blade in the bladed disk, N_B is the number of blades in the bladed disk, $\boldsymbol{F}_{nln}(\boldsymbol{x})$ is the vector of non-linear internal forces, $\boldsymbol{P}$ is the vector of static external forces

and the global stiffness matrix, $\boldsymbol{K}$ of the bladed disk is obtained by assembling the element stiffness matrices $\boldsymbol{k}^e$:

$$\boldsymbol{k}^e = \int_{V^e} \boldsymbol{B}^T \mathbf{E}' \boldsymbol{B} \, \mathrm{d}V^e, \; e = 1, \ldots, N_{el} \tag{8}$$

where, $\boldsymbol{B}$ is the strain-displacement matrix , V^e is the element volume and N_{el} is the total number of elements.

Eq.(7) is solved using Newton-Raphson iteration method:

$$\boldsymbol{x}_{k+1} = \boldsymbol{x}_k + \boldsymbol{J}\left(\boldsymbol{K}\boldsymbol{x}_k + \boldsymbol{F}_{nln}(\boldsymbol{x}_k) - \boldsymbol{P}\right) \tag{9}$$

where $\boldsymbol{J} = \left(\boldsymbol{K} + \frac{\partial \boldsymbol{F}_{nln}}{\partial \boldsymbol{x}}\right)$ is the Jacobian of Eq.(7) and $\boldsymbol{x}_k, \boldsymbol{x}_{k+1}$ are the approximate solutions obtained at k^{th} and $(k+1)^{\text{th}}$ iteration respectively. The iterative process terminates when the solution reaches sufficient accuracy, ε; for e.g. when $||\boldsymbol{x}_{k+1} - \boldsymbol{x}_k|| < \varepsilon$.

3.2 Calculation of displacement sensitivities

The equation for displacement sensitivity corresponding to j^{th} blade anisotropy is obtained by differentiating Eq.(7) w.r.t anisotropy orientation vector, $\boldsymbol{r}_j$:

$$\frac{\partial \boldsymbol{K}}{\partial \boldsymbol{r}_j}\boldsymbol{x} + \boldsymbol{K}\frac{\partial \boldsymbol{x}}{\partial \boldsymbol{r}_j} + \frac{\partial \boldsymbol{F}_{nln}}{\partial \boldsymbol{x}}\frac{\partial \boldsymbol{x}}{\partial \boldsymbol{r}_j} = 0 \tag{10}$$

rearranging terms in Eq.(10):

$$\left(\boldsymbol{K} + \frac{\partial \boldsymbol{F}_{nln}}{\partial \boldsymbol{x}}\right)\frac{\partial \boldsymbol{x}}{\partial \boldsymbol{r}_j} = \boldsymbol{J}\frac{\partial \boldsymbol{x}}{\partial \boldsymbol{r}_j} = -\frac{\partial \boldsymbol{K}}{\partial \boldsymbol{r}_j}\boldsymbol{x}^*, \; j = 1, \ldots, N_B \tag{11}$$

where $\boldsymbol{x}^*$ is solution vector obtained by solving Eq.(7), $\partial \boldsymbol{x}/\partial \boldsymbol{r}_j$ is the required sensitivities and N_B is the total number of blades in the bladed disk.

The sensitivities of the element stiffness matrix w.r.t crystal orientation is calculated from Eq.(12)

$$\frac{\partial \boldsymbol{k}^e}{\partial \boldsymbol{r}_j} = \int_{V^e} \boldsymbol{B}^T \frac{\partial \mathbf{E}'}{\partial \boldsymbol{r}_j} \boldsymbol{B} \, \mathrm{d}V^e \tag{12}$$

The sensitivities of element stiffness matrix is assembled using conventional FE assembling procedure to obtain the sensitivities of global stiffness matrix, $\partial \boldsymbol{K}/\partial \boldsymbol{r}_j$, in the right hand side of Eq.(11). The Jacobian matrix, $\boldsymbol{J}$ in Eq.(11) is evaluated while solving Eq.(7), and hence, the computational cost involved in calculation of sensitivities is kept to minimum. The sensitivities are calculated for all blades of interest in the bladed disk.

3.3 Polynomial chaos expansion

The idea behind PCE is to project the stochastic output $y(\boldsymbol{\xi})$ in the n-dimensional random space spanned by mutually orthogonal polynomial basis $\psi_i(\boldsymbol{\xi})$ which are functions of the n-dimensional random variable $\boldsymbol{\xi} = \{\xi_1, \xi_2, \ldots, \xi_n\}$. The output function, which can be displacement, stress or modal characteristics like natural frequency, could be expanded using PCE as shown in Eq.(13)

$$y(\boldsymbol{\xi}) = \sum_{i=0}^{\infty} c_i \psi_i(\boldsymbol{\xi}) \tag{13}$$

where, c_i are unknown coefficients in the expansion that need to be evaluated. For practical reasons, RHS of Eq.(13) could be truncated by limiting the total degree of the basis terms to p, resulting in a truncated PC expansion given by Eq.(14)

$$y(\boldsymbol{\xi}) \approx \sum_{i=0}^{P} c_i \psi_i(\boldsymbol{\xi}) \tag{14}$$

where, $P + 1 = (n+p)!/n!p!$. The orthogonality of the basis function w.r.t the probability distribution of the random variables implies that the inner product of the function satisfy Eq.(15)

$$\langle \psi_r(\boldsymbol{\xi}), \psi_s(\boldsymbol{\xi}) \rangle = \int_{\Omega} \psi_r(\boldsymbol{\xi}) \psi_s(\boldsymbol{\xi}) d\mu(\boldsymbol{\xi}) = \gamma_n \delta_{rs} \tag{15}$$

where, γ_n are constants, δ_{rs} is the Kronecker delta and $d\mu(\boldsymbol{\xi})$ is the probability measure in the n-dimensional random space given by Eq.(16) for statistically independent random variables

$$d\mu(\boldsymbol{\xi}) = \rho_1(\xi_1)\rho_2(\xi_2)\ldots\rho_n(\xi_n) d\xi_1 d\xi_2 \ldots d\xi_n \tag{16}$$

where, ρ_n is the probability density function of ξ_n. The choice of basis functions in Eq.(13) is based on the probability distribution of the random variables. Table 1 provides the choice of polynomial basis for few probability distributions of the random variables.

To calculate the unknown coefficients in PCE, point collocation method is used. Using point collocation method, the error in approximation of stochastic is reduced to zero at selected points, called collocation points (CPs), in the n-dimensional random space. Enforcing the condition that the residual vanishes at $\boldsymbol{\xi}_1, \ldots, \boldsymbol{\xi}_N$ provides a set of N linear algebraic equations in c_i, $i \in \{0, 1 \ldots, P\}$. When the number of realizations of the exact model is greater than the number of coefficients in Eq.(13), then the system of linear equations is overdetermined and is solved using least squares approach.

3.4 PCE using gradient information.

The number of terms in PCE increases exponentially as the dimension of random space increases, increasing the computational cost. This problem is often referred in the literature as the "curse of dimensionality". To address this curse-of-dimensionality problem, the use of gradient values in evaluating the coefficients of polynomial response surfaces for maximum amplitude of vibrations in mistuned bladed disks was proved to be very useful (see Ref.[23], [24]) For an n-dimensional random space, the number of linearly independent equations obtained by including gradient values is $(1+n)$ times the number of CPs

where n is the number of random variables. Therefore, the minimum number of model realizations required to obtain the coefficients in a polynomial approximation is reduced by a factor of $1/(1+n)$. The gradient values of output function evaluated at CPs are used to determine the coefficients of PCE:

$$\begin{bmatrix} \psi_0(\boldsymbol{\xi}_1) & \psi_1(\boldsymbol{\xi}_1)\dots\psi_P(\boldsymbol{\xi}_1) \\ \frac{\partial\psi_0(\boldsymbol{\xi}_1)}{\partial\xi_1} & \frac{\partial\psi_1(\boldsymbol{\xi}_1)}{\partial\xi_1}\cdots\frac{\partial\psi_P(\boldsymbol{\xi}_1)}{\partial\xi_1} \\ \vdots & \\ \frac{\partial\psi_0(\boldsymbol{\xi}_1)}{\partial\xi_n} & \frac{\partial\psi_1(\boldsymbol{\xi}_1)}{\partial\xi_n}\cdots\frac{\partial\psi_P(\boldsymbol{\xi}_1)}{\partial\xi_n} \\ \psi_0(\boldsymbol{\xi}_2) & \psi_1(\boldsymbol{\xi}_2)\dots\psi_P(\boldsymbol{\xi}_2) \\ \frac{\partial\psi_0(\boldsymbol{\xi}_2)}{\partial\xi_1} & \frac{\partial\psi_1(\boldsymbol{\xi}_2)}{\partial\xi_1}\cdots\frac{\partial\psi_P(\boldsymbol{\xi}_2)}{\partial\xi_1} \\ \vdots & \\ \psi_0(\boldsymbol{\xi}_N) & \psi_1(\boldsymbol{\xi}_N)\dots\psi_P(\boldsymbol{\xi}_N) \\ \vdots & \\ \frac{\partial\psi_0(\boldsymbol{\xi}_N)}{\partial\xi_n} & \frac{\partial\psi_1(\boldsymbol{\xi}_N)}{\partial\xi_n}\cdots\frac{\partial\psi_P(\boldsymbol{\xi}_N)}{\partial\xi_n} \end{bmatrix} \cdot \begin{Bmatrix} c_0 \\ c_1 \\ \vdots \\ c_P \end{Bmatrix} = \begin{Bmatrix} y(\boldsymbol{\xi}_1) \\ \frac{\partial y(\boldsymbol{\xi}_1)}{\partial\xi_1} \\ \vdots \\ \frac{\partial y(\boldsymbol{\xi}_1)}{\partial\xi_n} \\ y(\boldsymbol{\xi}_2) \\ \frac{\partial y(\boldsymbol{\xi}_2)}{\partial\xi_1} \\ \vdots \\ y(\boldsymbol{\xi}_N) \\ \vdots \\ \frac{\partial y(\boldsymbol{\xi}_N)}{\partial\xi_n} \end{Bmatrix} \quad (17)$$

where, $\psi_0(\boldsymbol{\xi}_1)$, $\psi_1(\boldsymbol{\xi}_1)$, …, $\psi_P(\boldsymbol{\xi}_1)$ are basis functions evaluated at first CP, c_0, c_1, …, c_P are deterministic coefficients in the polynomial expansion, and $y(\boldsymbol{\xi}_1),\dots,y(\boldsymbol{\xi}_N)$ are exact values of the output obtained by evaluations of mistuned bladed disk model at CPs. $\partial y(\boldsymbol{\xi}_i)/\partial\xi_j$ represents the gradient value of output w.r.t j^{th} random parameter evaluated at i^{th} CP.

TABLE 1: Choice of basis functions

Distribution	Polynomial	Basis terms
Normal $\mathcal{N}(0,1)$	Hermite	$\psi_0=1,\psi_1=\xi,\psi_2=\xi^2-1,$ $\psi_3=\xi^3-3\xi,$ $\psi_4=\xi^4-6\xi^2+3$
Uniform $\mathcal{U}(-1,1)$	Legendre	$\psi_0=1,\psi_1=\xi,$ $\psi_2=\xi^2-0.3333,$ $\psi_3=\xi^3-0.6\xi,$ $\psi_4=\xi^4-0.8571\xi^2+0.08571,$
Exponential	Laguerre	$\psi_0=1,\psi_1=\xi-1,$ $\psi_2=\xi^2-4\xi+2,$ $\psi_3=\xi^3-9\xi^2+18\xi-6,$ $\psi_4=\xi^4-16\xi^3+72\xi^2-96\xi+24$

For a multivariate output function, the polynomial basis are obtained as tensor products of orthogonal polynomials for corresponding univariate case. The dimension of the tensor product increases exponentially with increase in number of random parameters, and therefore, increases the number of model realizations required. In this study, a cross truncation feature available in *Chaospy* [25], a Python tool box for uncertainty quantification, is used to truncate the full tensor product set, a-priori, by ignoring some of the higher order interactions of variables in the orthogonal basis set.

4 FE MODEL OF BLADED DISK

The developed methodology has been applied to the analysis of a finite element model of a realistic bladed disk. The full model of the bladed disk is shown in Fig.1a. The blades are attached to disk using fir-tree root joints (Fig. 2b) and are connected through shrouds. The disk is made of isotropic material and the blades are made of single crystal material with face centred cubic structure. The axial and tangential degrees of freedom for nodes on the rim of the disk are constrained. Ten-node tetrahedral elements are used to create FE model of the bladed disk which has 0.5 million nodes. The FE mesh for the bladed disk is shown in the Fig. 2a. While linear bladed disks has bonded contacts at root and shroud, for non-linear bladed disks, face-to-face penalty frictional contact elements are used to define the contacts at root and shroud contact interfaces with friction coefficient values of 0.1 and 0.3 respectively. The total number of friction contact elements in the FE model of the bladed disk is 17475. Centrifugal load corresponding to the rotational speed of 8625 rpm is applied. The FE analysis is performed using *CalculiX* [26], which is an open source FE analysis package.

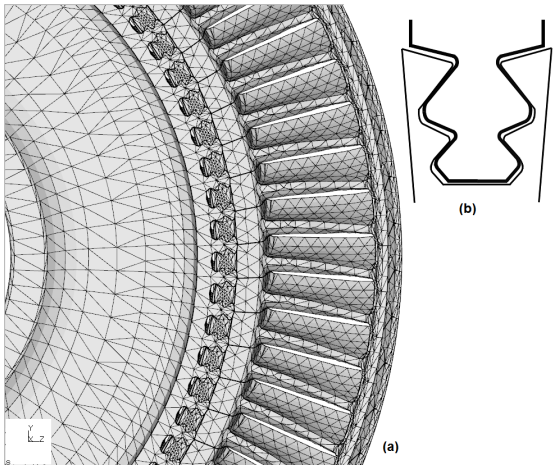

FIGURE 2: (a) FE mesh of bladed disk model and, (b) schematic diagram of fir-tree root geometry

5 RESULTS AND DISCUSSION

5.1 Local Sensitivity Analysis

Based on first order sensitivity, the effects of scatter in crystal orientation of blades on displacements and stresses in a mistuned bladed disk with (i) linear contacts and (ii) non-linear contacts at blade roots and shrouds are investigated.

5.1.1 Linear bladed disks. Models of linear bladed disks are considered as a special case of the more general analysis of non-linear bladed disks. The analysis performed for a linear bladed disk can provide valuable insights on the effects of anisotropy axis orientation on deformation of bladed disk at very low computational cost compared to that required for analysis of

non-linear bladed disks. In a linear bladed disk the blade roots and shroud contacts are assumed to be bonded contacts. Mistuning is introduced by choosing the material anisotropy angles, α, β and ζ, of each blade of the bladed disk randomly from the probability distributions for these angles provided by the manufacturer. An example of the distribution of blade anisotropy angles for all blades in the mistuned bladed disk is shown in Fig.3. In this plot, the values of blade angles are normalized due to confidentiality restrictions on the range of anisotropy angles obtained from the industry.

For the case of tuned bladed disk, with anisotropy axis aligned with blade stacking axis, and for mistuned bladed disk, Fig.4 and 5 shows the sensitivity of displacements at node A of blade#1 (Fig.1a) w.r.t anisotropy angles of all blades in the bladed disk. While maximum value of displacement sensitivity is obtained for tuned system, mistuning of bladed disks makes more number of blades influential in terms of displacement sensitivity. The sensitivity of blade displacements w.r.t the anisotropy angles α and β are higher as compared to anisotropy angle ζ. The sensitivity of axial displacement is higher which can be attributed to the absence of additional constraints which are imposed by the shrouds on other displacement components such as the tangential displacements. The sensitivity of displacements to anisotropy angles of blades decreases gradually as the position of blade gets farther from blade#1 in the bladed disk. It is clear from Fig.5 that anisotropy angles of blades located far from a considered blade shows little or no effects on the displacements of this blade.

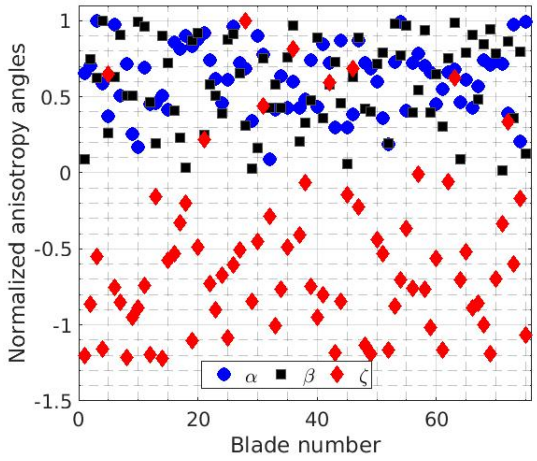

FIGURE 3: Normalized anisotropy angles for all blades in the mistuned bladed disk

5.1.2 Non-linear bladed disks. To estimate maximum scatter in blade displacements (worst case) due to material anisotropy based mistuning, 250 different mistuning patterns are analysed for non-linear and linear bladed disks. The displacements at blade tip of all 75 blades are considered across different mistuned bladed disks analysed. Table 2 shows maximum variation in axial, tangential and radial displacements at blade tip. The displacement components along axial and circumferential direction shows significant variation w.r.t scatter in anisotropy orientation. The maximum scatter of the blade displacements expressed in percents of values obtained for a tuned bladed disk is smaller for bladed disks with friction joints compared to bladed disks with bonded contacts.

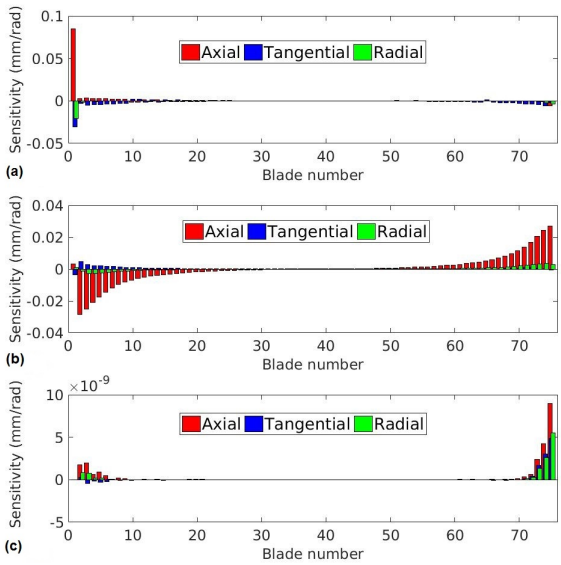

FIGURE 4: Sensitivity of displacements at tip node of blade#1 due to angle (a) α (b) β & (c) ζ in tuned linear bladed disk

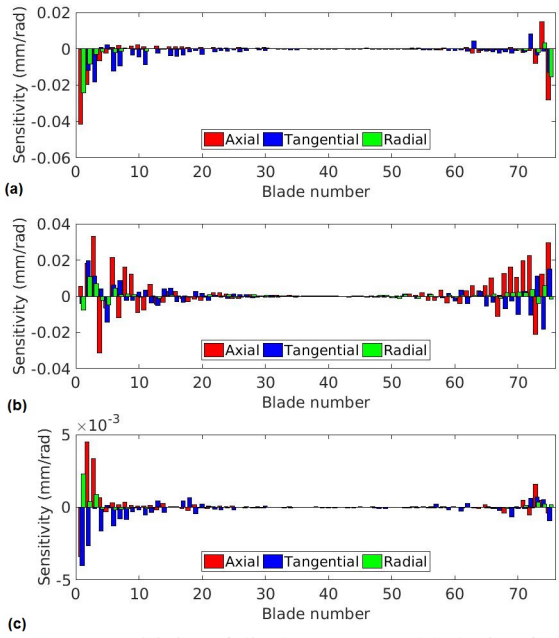

FIGURE 5: Sensitivity of displacements at blade tip of blade#1 to anisotropy angle (a) α (b) β and (c) ζ of all blades in a mistuned linear bladed disk

For mistuning pattern as shown in Fig. 3 the scatter in displacements at blade tip of individual blades in the bladed disk is shown in Fig.6. For the non-linear bladed disks studied, the variation in displacements along axial, circumferential and radial direction are 12%, 14% and 2.5%. Comparing with the variations of the linear bladed disk analysed, we can see that the scatter of displacements for the linear bladed disk are larger with respective values for axial, circumferential and radial displacement being 18%, 33% and 5%. The magnitude of blade displacements for non-linear bladed disk are higher compared to that of the linear bladed disk having the same mistuning pattern.

TABLE 2: Scatter of blade tip displacements based on 250 different mistuning patterns

Displacement component		Displacement (mm)		Maximum scatter (%)	
		linear	non-linear	linear	non-linear
Axial	Max.	0.3935	0.4107	84.4	18.3
	Min.	0.2134	0.3471		
Circumferential	Max.	0.1798	0.3282	110.9	20.6
	Min.	0.0853	0.2722		
Radial	Max.	0.6550	0.7794	7.2	3.1
	Min.	0.6107	0.7560		

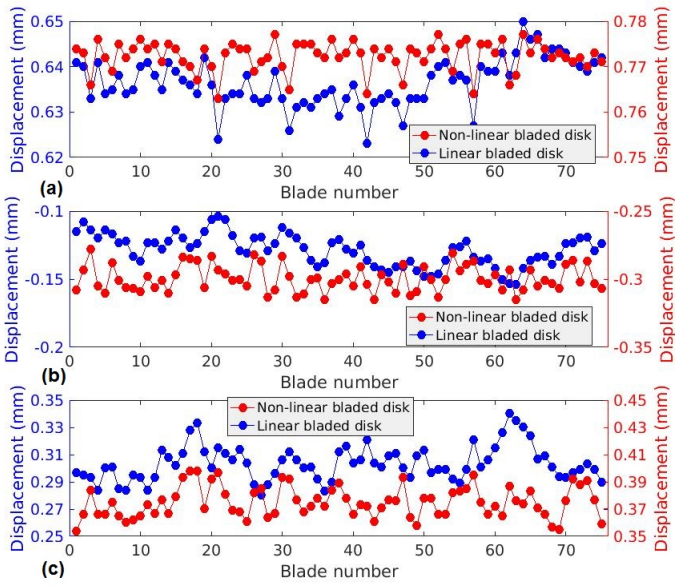

FIGURE 6: Displacements at blade tip of all blades in (a) radial (b) tangential & (c) axial direction in a mistuned bladed disk

The sensitivity of axial displacement w.r.t crystal orientation of blades is higher compared to that of tangential and radial components. As an example, the axial displacement and their sensitivities over the whole FE model of the bladed disk are displayed in Fig.7a for the mistuning pattern shown in Fig.3. The axial displacements has small differences from blade to blade which is not clearly discernible from the plot of displacements for the full bladed disk (Fig.7a). In order to highlight the scatter in axial displacements, zoomed view of several blades in the bladed disk

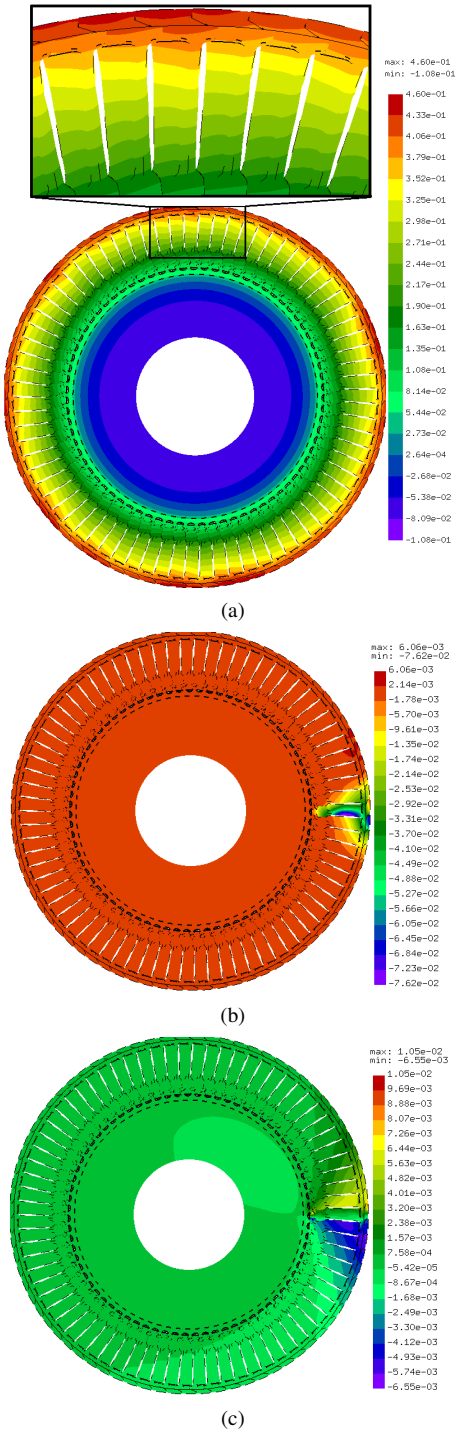

FIGURE 7: (a) Axial displacement and, its sensitivity to blade#1 anisotropy angles (b) α and (c) β in a mistuned bladed disk.

is shown in the inset in Fig.7a which clearly shows small differences in the axial displacements between adjacent blades.

Sensitivities of axial displacement to anisotropy angles α and β of blade#1 are shown in Fig. 7b and 7c respectively. While the crystal orientations of a blade influence the displacements of that blade and those in the immediate neighbourhood, its effect is negligible for blades positioned farther in the bladed disk. The sensitivity of axial displacement to anisotropy angle α is maximum at the leading edge towards mid-span of blade#1 and the maximum sensitivity to angle β occurs at blade tip region. As shown for the mistuned bladed disk studied and in general, the magnitude of displacement and stress sensitivities to anisotropy angles is maximum w.r.t anisotropy angle α. The sensitivity w.r.t third anisotropy angle ζ is an order of magnitude smaller than that of the first two angles.

The effects of variation in anisotropy angles of all blades in the bladed disk on stresses at fir-tree root of blade#1 is shown in Fig.8. Similar to the sensitivity of displacements in linear bladed disk, the effect of anisotropy angle α is marginally higher than that of β. It is evident that sensitivity of stresses to anisotropy angles of all other blades except that of blade#1 is negligible.

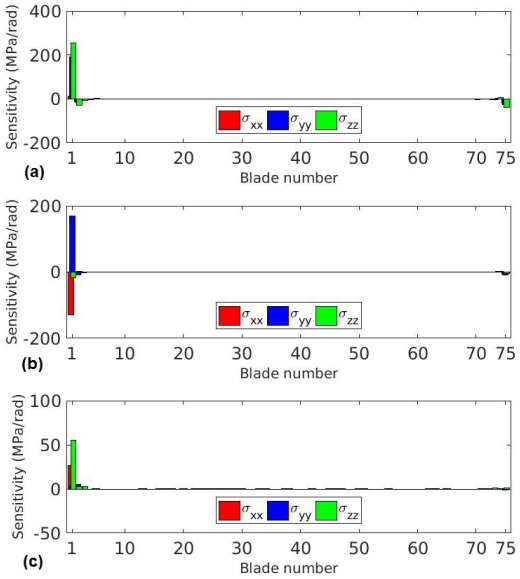

FIGURE 8: Sensitivity of stresses at blade root of blade#1 to anisotropy angle (a) α (b) β and (c) ζ of all blades in a mistuned bladed disk

5.2 Statistical analysis

The possibility of using polynomial chaos expansion to perform statistical analysis of mistuned bladed disk with linear and non-linear contacts is explored in this section. For this analysis crystal orientation of nine blades, labelled in Fig. 1a, are varied resulting in a total of 27 anisotropy angles as random variables. The choice of these nine blades is based on the following considerations, (i) local sensitivity analysis (Fig. 5) justifies the choice of few blades in the immediate neighbourhood of the blade for which the statistical characteristics are sought and, (ii) to reduce dimensionality of the problem by limiting the number of random variables. The PCE obtained for deformation of bladed disk is compared for the two cases, when coefficients of expansion are obtained from: (i) function evaluations and, (ii) function evaluations and gradient values. The authors use the term "gradPCE" to refer to polynomial chaos expansions when the expansion coefficients are evaluated from gradient values as well as function values at collocation points where as, henceforth, PCE will refer to polynomial chaos expansion when the coefficients are evaluated based on function values alone. The sampling of input parameter space is based on Sobol sequences which are effective in exploration of multidimensional space [27]. The present study uses *Chaospy* [25] to obtain polynomial chaos (PC) based statistics.

5.2.1 Linear bladed disk.

As a first step, for linear bladed disk, considering only the first two anisotropy angles of blade#1 as random variables the effectiveness of PC expansion in approximating displacements of blade#1 is investigated. The original variation in displacements are obtained from FE analysis of bladed disks by varying the anisotropy angles α and β of blade#1 from 0^0 to 15^0 and 0^0 to 90^0 respectively. The variations obtained for axial and radial displacement shows that displacements are more sensitive to anisotropy angle α over the entire domain. While the radial displacement is maximum for α equal to zero, which is the case when orientation of crystal axis is close to the blade stacking axis, the axial displacement is maximum for α equal to 15^0.

PC approximations of second degree for displacements at node A (Fig.1a) w.r.t the first two anisotropy angles of blade#1 in a mistuned bladed disk is shown in Fig.9. The expansion coefficients in PCE and gradPCE are calculated from 10 and 6 evaluations of mistuned bladed disk respectively. It is clear that the gradient based PC expansion provides a good approximation over most of the domain for the original variation of displacements obtained from FE model evaluations.

A PC expansion of degree 2 in terms of two random variables has 6 expansion coefficients. While the mean value of the distribution of stochastic output function is given by the first coefficient, the sum of squares of all the coefficients except the first gives the variance of the distribution. It is important to realize that the same approximation obtained using PC, i.e. using mutually orthogonal polynomial basis of n^{th} degree, could be obtained by using monomials of the random variables of upto n^{th} degree as basis functions. PC expansion allows easy estimation of statistical characteristics for the distribution of the stochastic output. Polynomial approximations obtained using monomial basis will necessitate additional steps such as MCS using this approximation to obtain the statistical characteristics.

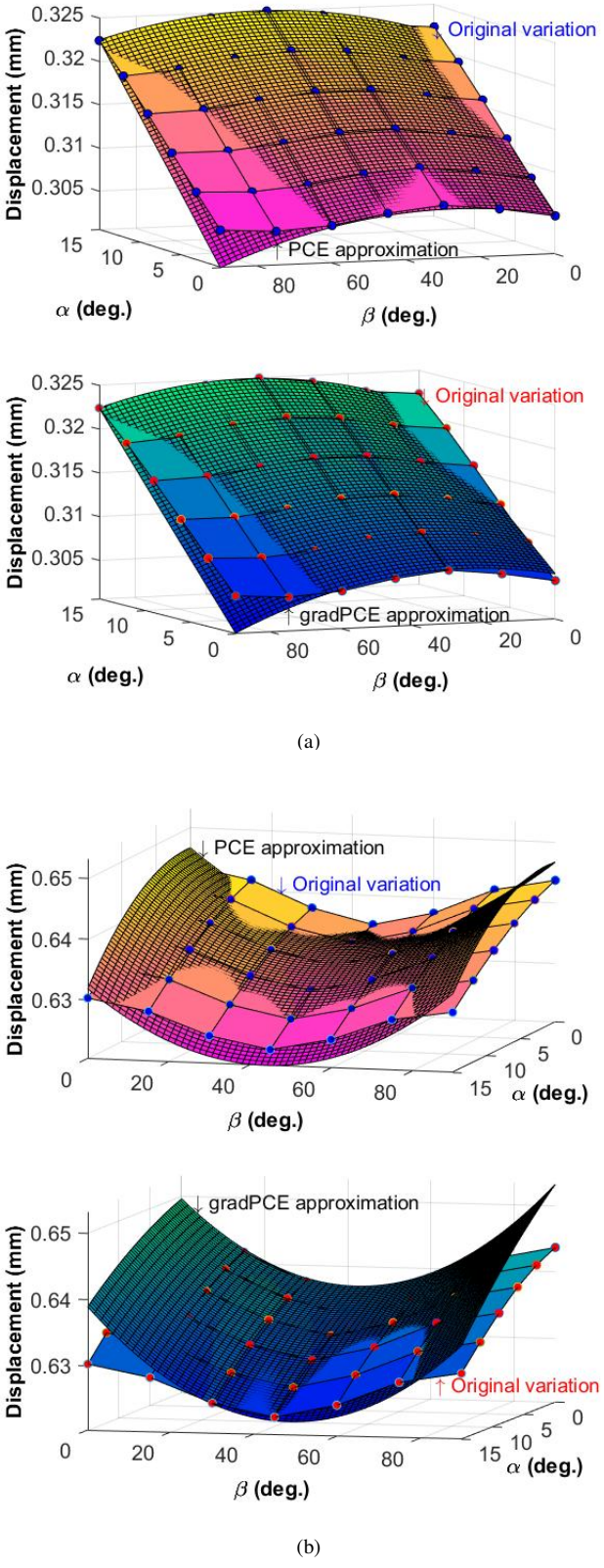

FIGURE 9: PCE and gradPCE approximations for (a) axial and (b) radial displacement at blade tip of blade#1

Table 3 compares the values for mean and STD of blade#1 tip displacements obtained using PCE and gradPCE to those obtained through MCS of 2850 evaluations of linear bladed disk model. For linear bladed disk analysed, increasing the degree of polynomial expansion from 2 to 3 provides no improvement in the statistics obtained using gradPCE. For the case of PCE, increasing the degree of PC expansion deteriorate the accuracy of statistics obtained. This behaviour could be explained by considering the ratio of number of collocation points used to the number of expansion coefficients, referred to as oversampling ratio (OSR) by Hosder et al.[28]. Compared to an over sampling ratio of approximately two used for PCE of degree 2, OSR of nearly one is used for PCE of degree 3. The more accurate statistics from the former case, confirms the observation made by Hosder et al.[28] regarding the better statistics obtained from PCE using an OSR of value two.

Further reduction in computational cost is achieved by ignoring higher order interaction terms in the basis set of PCE. Table 4 compares the statistics of displacements obtained using PCE of degree two with full basis set and the truncated basis set to results obtained using Monte Carlo simulation (MCS). For the problem studied, sufficiently accurate statistics can be obtained by using truncated basis set at a computational time as low as one-third of that required when using a full basis set.

To build surrogate models using PCE the gradient values are not needed, and therefore, the computational effort is spend only in evaluating the displacements from the FE model of bladed disks. For building the gradPCE based surrogate models additional computational effort is spend in calculating the gradient values of displacements. When the computational time for FE analysis is smaller than that required for calculating gradient values, as is the case for linear bladed disks, the advantage of using only fewer number of model evaluations for gradPCE method is offset by the additional time required for calculating gradient values. Therefore, for linear bladed disk models gradPCE offers no reduction in computational cost compared to PCE.

5.2.2 Non-linear bladed disk. The computational cost required for analysis of non-linear models are significantly higher than those required for linear models. Therefore the use of surrogate models that can replace high fidelity computational models is imperative. In this section, the statistical characteristics for response of a non-linear bladed disk is obtained using PC.

PC expansion of degree two in terms of anisotropy angles of the nine blades, shown in Fig.1a, as random parameters is obtained for deformation of non-linear bladed disk. For both PCE and gradPCE, truncated basis set is used, which results in the reduction of the number of terms in the expansion from 406 to 55. Fig. 10 shows the convergence of standard deviation for displacements at node A (Fig.1a), obtained from PCE and gradPCE, w.r.t to the number of non-linear bladed disk models evaluated to obtain the coefficients in the expansion.

TABLE 3: Statistics for blade#1 tip displacements obtained from polynomial chaos expansion and MCS

Degree of PC expansion	Number of coefficients in PC expansion	Number of evaluations		Displacement component	Mean (mm)			Standard deviation (mm)		
		grad-PCE	PCE		gradPCE	PCE	MCS	gradPCE	PCE	MCS
2	55	40	120	Axial	0.2990	0.3023	0.3017	0.0214	0.0280	0.0208
				Tangential	0.1405	0.1430	0.1442	0.0092	0.0095	0.0105
				Radial	0.6396	0.6396	0.6394	0.0109	0.0068	0.0098
3	433	90	460	Axial	0.2999	0.3026	0.3017	0.0188	0.0361	0.0208
				Tangential	0.1411	0.1435	0.1442	0.0112	0.0212	0.0105
				Radial	0.6402	0.6398	0.6394	0.0093	0.0138	0.0098

TABLE 4: Statistics for displacements of blade#1 of a linear mistuned bladed disk

Type of PC basis	Number of coefficients	Number of evaluations of bladed disk	Model evaluation time (hrs)	Displacement component	Mean (mm)		Standard deviation (mm)	
					PCE	MCS	PCE	MCS
Full	406	410	34	Axial	0.3011	0.3017	0.0970	0.0208
				Tangential	0.1446	0.1442	0.0322	0.0105
				Radial	0.6397	0.6394	0.0329	0.0098
Truncated	55	120	10	Axial	0.3023	0.3017	0.0280	0.0208
				Tangential	0.1430	0.1442	0.0095	0.0105
				Radial	0.6396	0.6394	0.0068	0.0098

For the non-linear bladed disk model gradPCE is used to calculate the statistical parameters for scatter in displacements with an accuracy of two decimal places. Table 5 gives the statistics for displacements at blade tip of blade#1 in a non-linear mistuned blade disk with random crystal orientations for 9 blades as shown in Fig.1a. While the mean and standard deviation obtained using PCE and gradPCE from 105 FE realizations have close correspondence, the corresponding values obtain using 60 realizations differ especially for standard deviation. For gradPCE, the number of linearly independent equations obtained is much higher than the number of expansion coefficients, and hence, the statistics obtained from PC are less dependent on the number of mistuned bladed disk evaluated. Therefore, gradPCE requires less model evaluations compared to that required for PCE and hence reduces the computational cost involved in calculating mean and standard deviation.

The proposed gradPCE method is shown to achieve fast convergence for STD of displacements w.r.t model evaluations for non-linear bladed disks analysed. Therefore, it reduce the computational cost for calculating displacement statistics for non-linear bladed disks from 271 hrs (105 model evaluations required for PCE) to 185 hrs (60 model evaluations).

6 SOME IMPLICATIONS OF THE RESULTS

The analysis of non-linear bladed-disks based on several mistuning patterns (Table 2) shows that a maximum displacement scatter of 21% and 18% is possible in circumferential and axial direction due to scatter in blade material anisotropy orientation. This underlines the need to account for displacement scatter while determining clearance values for bladed disks in high pressure turbine stages of gas turbines.

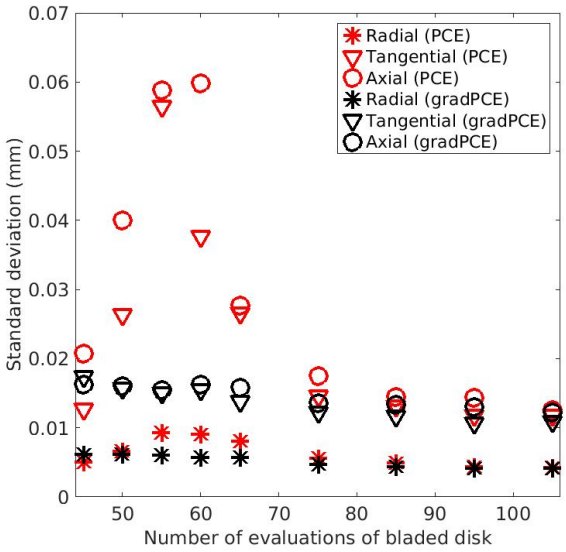

FIGURE 10: Standard deviation for displacements w.r.t number of evaluations of mistuned bladed disk

TABLE 5: Statistics for displacements of blade#1 for a mistuned non-linear bladed disk

Number of coefficients in PC expansion	Model evaluations	Model evaluation time		Displacement	Mean		STD	
		PCE	gradPCE		PCE	gradPCE	PCE	gradPCE
		(hrs)	(hrs)		(mm)	(mm)	(mm)	(mm)
55	60	155	185	Axial	0.3754	0.3747	0.0598	0.0162
				Tangential	0.2946	0.2948	0.0376	0.0155
				Radial	0.7766	0.7764	0.0091	0.0058
	105	271	323	Axial	0.3757	0.3756	0.0126	0.0122
				Tangential	0.2945	0.2945	0.0118	0.0109
				Radial	0.7763	0.7763	0.0042	0.0042

In order to obtain the scatter in blade tip displacements across all 75 blades in the bladed disk, 250 different linear and non-linear mistuned bladed disks with random anisotropy angles for all 75 blades were studied. The results from this study (see Table 2) shows significant scatter in blade displacements over all blades, for example, displacements in circumferential direction have maximum variation of 110.9% & 20.6% for linear and non-linear bladed disks respectively. On the contrary, while studying scatter in displacements for one blade, the values for STD in blade displacements obtained from statistical analysis based on random anisotropy angles of only 9 blades indicates marginal scatter (see Table 3 & 5). For instance, tangential displacements have maximum variation of 6.9% & 3.7% for linear and non-linear bladed disks respectively. This points to the importance of accounting for randomness in anisotropy angles of all blades in the bladed disk while performing the statistical analysis.

Sensitivities obtained from the LSA identify the anisotropy angles that contribute significantly to variation in displacements of a particular blade. Therefore, sensitivity analysis provides valuable information that can be used to confine the scatter in displacements within desired limits by controlling the parameters in casting process of single crystal blades in order to limit the scatter in certain anisotropy angle.

The scatter in blade displacements due to uncertainty in anisotropy orientations will result in different shroud contact conditions at different blades in the bladed disk which will in-turn influence the dynamic properties of bladed disks, the extend of which must be determined through further investigations.

7 CONCLUSIONS

Efficient methods for LSA and statistical analysis of mistuned bladed disks with random blade material anisotropy orientations have been developed. The local sensitivity analysis method allows the efficient calculation of sensitivities for deformation and stress fields in mistuned bladed disks w.r.t crystal orientations of single crystal blades for the following two cases, (a) linear bladed disks with bonded contacts and, (b) non-linear bladed disks with friction joints at blade roots and shrouds.

The analysis was performed to obtain statistical characteristics of bladed disk response using PC expansion.Two approaches are used to address the curse of dimensionality problem which are: (a) use of gradient values to calculate expansion coefficients in PC and, (b) basis truncation for multivariate PC. It is demonstrated that the use of gradPCE ensures faster convergence for statistical characteristics of bladed disk response.

Numerical studies of realistic, high fidelity bladed disk models have been performed to demonstrate the efficiency of the proposed methods. For linear bladed disks, the statistical characteristics for deformation under centrifugal load, w.r.t scatter in blade material anisotropy orientation, obtained from PC expansion are compared with those obtained from MCS. The comparison shows good correspondence for the gradPCE which predicts the mean and STD for displacements with sufficient accuracy.

For the non-linear bladed disks analysed it has been observed that faster convergence for displacement statistics could be obtained when gradient values are used to calculate polynomial expansion coefficients, along with function values, thereby reducing the computational cost significantly.

ACKNOWLEDGEMENT

The authors gratefully acknowledge the financial and technical support provided by MTU Aero Engines AG, Germany.

REFERENCES

[1] Segersäll, M., Leidermark, D., and Moverare, J. J., 2015. "Influence of crystal orientation on the thermomechanical fatigue behaviour in a single-crystal superalloy". *Materials Science and Engineering: A,* ***623***, pp. 68 – 77.

[2] Bounazef, M., Guessasma, S., and Bedia, E. A. A., 2007. "Blade protection and efficiency preservation of a turbine by a sacrificial material coating". *Advanced Powder Technology,* ***18***(2), pp. 123 – 133.

[3] Kaneko, Y., 2011. "Study on vibration characteristics of single crystal blade and directionally solidified blade". In *Proc. of the ASME Turbo Expo*. GT2011-45032. Vancouver, Canada, June 6-10, 2011.

[4] Manetti, M., Giovannetti, I., Pieroni, N., Horculescu, H., Peano, G., Zonfrillo, G., and Giannozzi, M., 2009. "The dynamic influence of crystal orientation on a second generation single crystal material for turbine buckets". In *Proc. of the ASME Turbo Expo*. GT2009-59091. Orlando, Florida, USA, June 8–12, 2009.

[5] Wen, Z., Mao, H., Yue, Z., and Wang, B., 2014. "The influence of crystal orientation on vibration characteristics of dd6 nickel-base single crystal superalloy turbine blade". *Journal of Materials Engineering and Performance,* ***23***(2), pp. 372–377.

[6] Savage, M., 2012. "The influence of crystal orientation on the elastic stresses of a single crystal nickel-based turbine blade". *Journal of Engineering for Gas Turbines and Power,* ***134***(1).

[7] Arakere, N., and Swanson, G., 2002. "Effect of crystal orientation on fatigue failure of single crystal nickel base turbine blade superalloys". *Journal of Engineering for Gas Turbines and Power,* ***124***(1), pp. 161–176. cited By 93.

[8] Weiss, T., Voigt, M., Schlums, H., Mücke, R., Becker, K.-H., and Vogeler, K., 2009. "Probabilistic finite-element analyses on turbine blades". In *Proc. of the ASME Turbo Expo*. GT2009-59877. Orlando, Florida, USA, June 8–12, 2009.

[9] Saltelli, A., and Scott, M., 1997. "Guest editorial: The role of sensitivity analysis in the corroboration of models and itslink to model structural and parametric uncertainty". *Reliability Engineering & System Safety,* ***57***(1), pp. 1 – 4.

[10] Petrov, E., 2009. "Analysis of sensitivity and robustness of forced response for nonlinear dynamic structures". *Mechanical Systems and Signal Processing,* ***23***(1), pp. 68–86.

[11] Petrov, E., 2008. "A sensitivity-based method for direct stochastic analysis of nonlinear forced response for bladed disks wirh friction interfaces". *Journal of Engineering for Gas Turbines and Power,* ***130***(2).

[12] Panunzio, A. M., Salles, L., Schwingshackl, C., and Gola, M., 2015. "Asymptotic numerical method and polynomial chaos expansion for the study of stochastic non-linear normal modes". In *Proc. of the ASME Turbo Expo*. GT2015-43560. Montreal, Cananda, June 15-19, 2015.

[13] Sinha, A., 2006. "Computation of the statistics of forced response of a mistuned bladed disk assembly via polynomial chaos". *Journal of Vibration and Acoustics, Transactions of the ASME,* ***128***(4), pp. 449–457.

[14] Pauw, D. J. D., and Vanrolleghem, P. A., 2006. "Practical aspects of sensitivity function approximation for dynamic models". *Mathematical and Computer Modelling of Dynamical Systems,* ***12***(5), pp. 395–414.

[15] Hsieh, C., and Arora, J., 1984. "Design sensitivity analysis and optimization of dynamic response". *Computer Methods in Applied Mechanics and Engineering,* ***43***(2), pp. 195 – 219.

[16] Brüls, O., and Eberhard, P., 2008. "Sensitivity analysis for dynamic mechanical systems with finite rotations". *International Journal for Numerical Methods in Engineering,* ***74***(13), pp. 1897–1927.

[17] Helton, J. C., 1993. "Uncertainty and sensitivity analysis techniques for use in performance assessment for radioactive waste disposal". *Reliability Engineering & System Safety,* ***42***(2), pp. 327 – 367.

[18] Allaire, D. L., and Willcox, K. E., 2012. "A variance-based sensitivity index function for factor prioritization". *Reliability Engineering & System Safety,* ***107***, pp. 107 – 114. SAMO 2010.

[19] Arregui-Mena, J. D., Margetts, L., and Mummery, P. M., 2016. "Practical application of the stochastic finite element method". *Archives of Computational Methods in Engineering,* ***23***(1), Mar, pp. 171–190.

[20] Blatman, G., and Sudret, B., 2010. "Efficient computation of global sensitivity indices using sparse polynomial chaos expansions". *Reliability Engineering & System Safety,* ***95***(11), pp. 1216 – 1229.

[21] Mezić, I., and Runolfsson, T., 2008. "Uncertainty propagation in dynamical systems". *Automatica,* ***44***(12), pp. 3003 – 3013.

[22] West, T., and Gumbert, C., 2017. "Multifidelity, multidisciplinary design under uncertainty with non-intrusive polynomial chaos". *58th AIAA/ASCE/AHS/ASC Structures, Structural Dynamics, and Materials Conference*.

[23] Petrov, E., Vitali, R., and Haftka, R., 2000. "Optimization of mistuned bladed discs using gradient-based response surface approximations". *41st Structures, Structural Dynamics, and Materials Conference*.

[24] Roderick, O., Anitescu, M., and Fischer, P., 2010. "Polynomial regression approaches using derivative information for uncertainty quantification". *Nuclear Science and Engineering,* ***164***(2), pp. 122–139.

[25] Feinberg, J., and Langtangen, H. P., 2015. "Chaospy: An open source tool for designing methods of uncertainty quantification". *Journal of Computational Science,* ***11***(Supplement C), pp. 46 – 57.

[26] Dhondt, G., 2017. "CalculiX CrunchiX user's manual version 2.12". In URL http:www.dhondt.de/ccx_2.12.pdf.

[27] Saltelli, A., Annoni, P., Azzini, I., Campolongo, F., Ratto, M., and Tarantola, S., 2010. "Variance based sensitivity analysis of model output. design and estimator for the total sensitivity index". *Computer Physics Communications,* ***181***(2), pp. 259 – 270.

[28] Hosder, S., Walters, R., and Balch, M., 2007. "Efficient sampling for non-intrusive polynomial chaos applications with multiple uncertain input variables". In *48th AIAA/ASME/ASCE/AHS/ASC Structures, Structural Dynamics and Materials Conference*. AIAA 2007-1939. Hawaii, Honolulu, 23-26 April, 2007.